Journal of Elementology ISSN 1644-2296

Mielnik, L., Tomaszewicz, T., Chudecka, J., Tomaszewicz, E., Podlasiński, M. and Hewelke, E. (2024)
'Spectroscopic properties of water soluble organic matter in artificial soil formed at a power plant from slag-ash deposits',
Journal of Elementology, 29(4), 1047-1065,
available: https://doi.org/10.5601/jelem.2024.29.3.3386

RECEIVED: 15 July 2024
ACCEPTED: 24 November 2024

ORIGINAL PAPER

Spectroscopic properties of water soluble organic matter in artificial soil formed at a power plant from slag-ash deposits*

Lilla Mielnik[1], Tomasz Tomaszewicz[2], Justyna Chudecka[2], Elżbieta Tomaszewicz[3], Marek Podlasiński[2], Edyta Hewelke[4]

[1] Department of Bioengineering
[2] Department of Environment Management
[3] Department of Organic and Analytical Chemistry
West Pomeranian University of Technology in Szczecin, Szczecin, Poland
[4] Institute of Environmental Engineering
Warsaw University of Life Sciences, Warsaw, Poland

Abstract

This study presents an evaluation of the properties of water extractable organic matter (WEOM) contained in anthropogenic soils, formed by superimposing four types of surface layers (0-40 cm) containing mixtures of organic and mineral waste on ash-slag mixture (the subsoil) left after coal combustion. After 12 years, selected properties of topsoil and subsoil horizons were analyzed. The topsoil had the texture of sand and loamy sand, conducive to water filtration. It was rich in organic matter, its pH was neutral or slightly alkaline, and its C:N ratio was usually optimal for soil organisms. The subsoil (40-60 cm) was strongly alkaline and often had the texture of loam, restricting water filtration. The WEOM fraction was evaluated by UV-Vis spectroscopy, fluorescence and delayed luminescence in order to disclose the variety of structural properties, which enabled an evaluation of its potential migration properties into the profile. The WEOM studied is poorly humified, which was predicable because of the short duration of the process (12 years). Structurally simple particles of low molecular mass are preferentially transported deeper into the ash-slag layer. Also, local activity of microbes and release of dissolved organic matter (DOM) from plant root excretion may be the sources of a large contribution of WEOM in ash-slag subsoils. WEOM components of greater molecular mass are retained in surface layers. WEOM transportation into the soil profile depends on the type of organic material, chemical and mineral components of different layers. The addition of ash significantly limits soil permeability, while bark is a sorbent of water including water-dissolved substances.

Keywords: fluorescence, luminescence spectroscopy, powder X-ray diffraction technique

Lilla Mielnik, PhD DSc, prof. ZUT, Department of Bioengineering, West Pomeranian University of Technology in Szczecin, Papieża Pawła VI 3, 71-459 Szczecin, Poland, e-mail: lmielnik@zut.edu.pl

* The work was financed from the funds for maintaining the research potential of the WKŚiR ZUT in Szczecin.

INTRODUCTION

It is estimated that coal combustion provides about 30% of total electric energy worldwide and the use of coal is anticipated to increase to 46% until 2030 (Yao et al. 2014). One of the main environmental problems related to coal use is how to handle coal combustion products (CCP), including mainly fly and bottom ashes and boiler slags. In Poland, coal combustion is the main source of energy and about 338 million tons of CCP had been collected on dumping grounds by the end of 2020 (Szawlec et al. 2022).

CCP may be used, either alone or as a component of certain materials, as stabilized and granulated foundations, embankments, construction filling and mine embankments for liquidation of coal pits and bores (Shon et al. 2009, Pierzyna 2017).

CCP have also been used in agriculture for soil fertility improvement, as they are a source of nutrients for plants, neutralize acidity, increase sorption capacity and microbiological activity of soils and reduce metal toxicity. Fly ashes improve physical properties of soil through reduction of their density and increase in their retention (Shaheen et al. 2014, Singh et al. 2016, Pandey 2020). CCP are also used for recultivation, including the formation of anthropogenic soils and introduction of plants onto devastated land, e.g. post-mining areas (Skousen et al. 2012).

The amounts of recycled CCP have increased in the last few decades, yet considerable quantities of these products remain deposited on dumping grounds, where they are hazardous to living organisms. Coal combustion products, and coal fly ash (CFA) in particular, have been classified as problematic solid waste, mainly because of the content of potentially toxic elements (PTE), as Cd, Cr, Ni and Pb, as well as organic compounds, e.g. PCBs, PAHs (Shahen et al. 2014, Yao et al. 2014, Khan, Umar 2019).

The most economic and ecological solution proposed so far is growing plants on landfills. Stabilization by plants curbs the weathering effect and leads to gradual recultivation of the land, limits leaching of different substances by water, results in the immobilization and bioaccumulation of metals, helps carbon sequestration, and has a positive impact on the landscape aesthetic value (Belyaeva, Haynes 2012, Pandey 2012). Colonization of CCP dumps by plants is slow because of undesirable properties of these waste products, such as the unfavorable air to water ratio, the tendency towards cementation, toxicity of heavy metals, strong alkaline pH, high salinity and poor accessibility of basic nutrients. Coal combustion products contain little or no nitrogen, phosphorus and carbon (Shaheen et al. 2014). These poor qualities may be improved by addition of organic waste materials such as sludge, natural fertilizers, composts to the upper layers, which increases the chance of successful recultivation and appearance of plants (Haynes 2009, Belayaeva, Haynes 2012). Addition of organic material enriches

CCP in carbon, nitrogen and phosphorus, increases bioavailability of organic nutrients, and reduces the accessibility of PTE; it also leads to neutralization of pH, reduction of salinity, stimulation of microbiological activity, and improvements of CCP physical properties (Ram, Masto 2014, Weber et al. 2015).

Organic matter (OM) is one of the main determinants of soil fertility and the cycling of particular elements in soil profiles. Its properties depend on the type of the initial material and conditions of humification and mineralization (Gaskin 2020, Gerke 2022, Waldrip et al. 2022). Dissolved organic matter (DOM) contains a number of non-uniform components and is the most reactive fraction of the OM pool in the soil. Its instability makes it the most mobile fraction, probably being most engaged in the biochemical processes occurring in the soil, hence it determines the availability of nutrients, complexation with ions, sorption on the soil surface, and participation in the carbon cycle (Zsolnay et al. 1999, Xu et al. 2013, Gao et al. 2017, Waldrip et al. 2022). In the soil, DOM is a complex mixture of organic compounds originating mainly from decomposition of plants, biomass of microbes and plant root secretions (Xu et al. 2013). It is a relatively easily decomposing fraction of soil OM with a high degree of biological circulation (Rees, Parker 2005). Its main components are carbohydrates and proteins, but it also contains aliphatic and aromatic components (Kaiser, Guggenberger 2000, Zhang et al. 2022). According to the rate of biodegradability, the components of DOM may be divided into two fractions: one with a high rate of biodegradability (the labile fraction), and the other one with a low biodegradability rate (the resistant fraction). The liable fraction includes simple carbohydrates, organic acids and proteins of low molecular mass. The resistant fraction contains the compounds present in micro- and mesopores, such as polysaccharides from decomposition of cellulose and hemicellulose, and other degradation products of microbiological origin (Bolan et al. 2011).

The methods commonly used for DOM characterization are UV-Vis and fluorescence spectroscopy (Zsolnay et al. 1999, Wei et al. 2014, Daouk et al. 2015, Gao 2018, He et al. 2021). Another photoluminescence method worth mentioning in the aspect of DOM characterization is that of delayed luminescence (DL) of OM. In this method, the DL intensity is measured at a certain time after cessation of irradiation of the material studied (Prokowski, Mielnik 2012, Mielnik, Asensio 2018).

The aim of the study was to evaluate the properties of WEOM collected from anthropogenic soils obtained by superimposing four types of surface layers that contained organic and mineral waste (0-40 cm), corresponding to the humus horizon, onto ash-slag mixture coming from coal combustion. Selected properties of the surface layers and ash-slag subsoil allowed us to assess the properties of WEOM and determine the soil condition.

MATERIALS AND METHODS

Research material

The object of the research was anthropogenic soil created on the premises of the Dolna Odra Power Plant in Nowy Czarnów (Poland, West Pomeranian voivodeship; 53,20°N, 14,48°E), as part of an experiment on the use of ash-slag left after coal combustion for soil regeneration and recultivation.

The soils were formed by deposition of a 40 cm fertile surface layer (S) on the subsoil material of post-coal combustion dump (A). Four variants of the fertile layer were used (SI–SIV) differing in composition and source of OM (Table 1). The soil was sown with a mixture of grass species – *Festuca rubra*, *Lolium perenne*, *Poa pratensis* (Czyż, Kitczak, 2007). After 12 years, soil samples were collected from the four variants of surface 0-40 cm layers (SI–SIV) and subsoil 40-60 cm layers of ash-slag (AI–AIV).

Table 1

The compositions of surface layers (S 0-40 cm) used in the experiment in the Dolna Odra Power Plant in Nowy Czarnów

Surface layer No.	Composition of surface layers
SI	loose sand, compost produced with GWDA method[#], coniferous wood bark, ash – ratio 1:2:1:4
SII	loose sand, compost produced with GWDA method, fermented municipal sewage sludge (dry weight: 70% sewage sludge, 15% straw, 15% urban green waste) – ratio 1:1:2
SIII	loose sand, compost produced with GWDA method, ash, fermented municipal sewage sludge (dry weight: 70% sewage sludge, 30% urban green waste) – ratio 1:2:1:4
SIV	loose sand, compost produced with GWDA method, coniferous wood bark, fermented municipal sewage sludge (dry weight: 70% sewage sludge, 30% straw) – ratio 1:2:1:4

[#] GWDA method – composting sludge with structural material using the static method with forced aeration.

Chemical and physical analysis

Soil physical and chemical analysis

The collected samples, after air drying, were characterized according to the following properties:

- texture by the Casagrande's method with Prószyński modifications, in complaince with WRB 2022;
- pH in 1 mol KCl dm^{-3} (pH_{KCl}) by the potentiometric method (a pH-meter Orion Star A 211);
- total carbon (TC) and total nitrogen (TN) using an elemental CHNS analyzer (Costech Instruments Elemental Combustion System);

– total organic carbon content (TOC) was calculated by subtracting the amount of carbon contained in calcium carbonate ($CaCO_3$) from the total carbon content (TC);
– $CaCO_3$ content using the Scheibler method.

XRD analysis of surface layers and ash-slag subsoils samples

Powder X-ray diffraction patterns of the samples labeled as surface layers SI–SIV and ash-slag subsoils AI–AIV were recorded at room temp. in the range of 10-100° 2Theta with the scanning rate of 0.013° per step on a EMPYREAN II diffractometer (PANalytical) using $CuK_{\alpha 1,2}$ radiation (λ = 1.5418 Å). Collected diffraction patterns were analyzed by a HighScore-Plus 4.0 software and used to determine composition of samples under study.

Water extraction procedure of organic matter

The solutions of WEOM were prepared by dissolving of 100 g air-dried soil in 1 dm^3 doubly distilled water (v/v 1:10) and were shaken on an orbital shaker for 24 h, at room temperature (20°C). The suspensions were centrifuged at 4000 rev min^{-1} for 20 minutes. Then, each WEOM sample was pre-filtered through a syringe filter with 0.45 μm pore size. In the filtrates, the amount of organic carbon (WEOC) and dissolved total nitrogen (WETN) were determined using an elemental CHNS analyzer (Costech Instruments Elemental Combustion System).

Characteristics of the extracted dissolved organic matter

UV-Vis spectroscopy

The analysis of spectral absorption in the UV-Vis range was performed using a UV-Vis-NIR Jasco 770 spectrophotometer. All spectra were recorded in the wavelength range from 220 to 760 nm, and were referenced to a blank spectrum of distilled water, at a constant room temperature. The absorption spectra obtained were used for the calculation of the following optical parameters: $SUVA_{254}$, E_{254}:E_{365} and ΔlogK, on the basis of absorbance at a certain wavelength.

Fluorescence spectroscopy

Fluorescence spectra were recorded on a Hitachi F 7000 fluorescence spectrophotometer, using a non-fluorescent quartz cuvette with the path length of 1 cm. The EEM were scanned by emission wavelengths from 250 nm to 600 nm and by excitation wavelengths from 200 to 500 nm. The spectra were recorded at the scan speed of 1200 nm min^{-1}, with an interval between the excitation and emission wavelengths of 10 nm, at room temperature. Correction of the spectra for instrumental response was performed according to the procedure recommended by Hitachi (Hitachi F 7000 Instruction Manual). In order to minimize the effect of the internal filter, the fluorescence spectra were recorded in a reflection system. The fluorescence spec-

tral data were used for the calculation of the following parameters: HIX, BIX, f_{450}/f_{500} and $\Sigma IFl_{465}/a_{465}$.

Delayed photoluminescence

Measurements of the excitation and registration of photoinduced luminescence intensity were taken with a flow set for continuous recording of the photoinduced luminescence of liquids and suspension. The device was constructed at the Department of Physics and Agrophysics West Pomeranian University of Technology in Szczecin (Prokowski, Mielnik 2012). DL was induced by light of wavelength λ_{ex} = 465-485 nm (DL-blue) and λ_{ex} = 620-630 nm (DL-red) with a photon flux density of 1,500 PAR μmol m^{-2} s^{-1}. The DL intensity was recorded at 0.10÷0.35 s after excitation. The time of recording corresponds to the time of flow of a given WEOM solution through the spiral cuvette in front of the photocathode of the measuring probe. The flow rate was 800 cm^3 min^{-1}. The spectral range of work of the photomultiplier recording the DL intensity was 185-850 nm The measurements were performed at a constant temp. of 25°C.

Graphical methods

The results obtained from UV-Vis, fluorescence and DL measurements were processed in MS Excel 2010. The figures generated in MS Excel were modified by CorelDRAW Graphics Suite 2021 for Windows Corporate. The resolution of EEM spectra was additionally refined by Quantum GIS version 3.10 using TIN interpolation. The spectra were smoothed in particular rasters using a resampling filter in SAGA GIS, with a rescale coefficient of 4. Comparison of the actual observations and results of estimations proved the consistence of results at a level of 96.0÷99.5%.

RESULTS AND DISCUSSION

Texture and chemical properties of surface layers (S) and ash-slag subsoils (A)

Although 4 different types of surface layers were used, they all (SI–SIV) have similar texture of sand and loamy sand, with clear dominance of sand fraction (78-91%) and no or very little of clay fraction, up to 2.5% (Table 2). Materials of such texture permit easy transportation of water suspensions and water enriched in different substances, including organic compounds, towards the ash-slag layer (Šulc et al. 2022). The ash-slag subsoils were characterized by greater diversity of texture; the AI–AIII indicated sandy loam and silt loam textural classes, while AIV was loamy sand. Diversity of the granulation of ashes and slag on disposal sites is a natural consequence of the randomness of deposition of these wastes and combustion

Table 2

The texture of surface layers (S) and ash-slag subsoils (A) according to WRB (2022)

Type	Fraction			Texture
	sand	silt	clay	
	(%)			
Surface layers				
SI	77.8	19.7	2.5	loamy sand
SII	87.9	9.9	2.2	sand
SIII	84.1	15.9	0.0	loamy sand
SIV	90.8	9.2	0.0	sand
Ash-slag subsoils layers				
AI	52.0	43.0	5.0	sandy loam
AII	58.0	39.5	2.5	sandy loam
AIII	43.5	54.5	2.0	silt loam
AIV	71.0	28.5	0.5	loamy sand

of coal batches of different compositions (Weber et al. 2015, Uzarowicz et al. 2017).

The pH_{KCl} values obtained for surface layers SII–SIV corresponded to neutral conditions; however, the value for SI, formed with a great contribution of ash (50 vol.%, Table 3) was alkaline. The lower values of pH_{KCl} of surface layers, relative to those of ash-slag subsoils, are a consequence of non-alkaline components (including OM) of the former. Neutral pH is optimum for most plants, while all ash-slag subsoils were strongly alkaline (Table 3). The pH values of combustion products usually vary in the range 6-11 (Skousen et al. 2012, Ram, Masto 2014, Singh et al. 2016) because they contain large amounts of calcium and magnesium oxides (Yao et al. 2014, Korotkova et al. 2017). Formation of calcium carbonates, mainly calcite, as a result of carbonation of CaO present in ash, is the most pronounced consequence of weathering, while an increase in the content of $CaCO_3$ is an indicator of pedogenesis progress (Uzarowicz et al. 2017). The content of calcium carbonate in ash-slag subsoils varied from 2.4 to 3.2%, and its increase indicated progressing weathering and considerable resistance to acidification of the subsoils.

The content of carbon in surface layers SII–SIV varied from 3.11 to 4.77% (Table 3), hence it was close to that in the humus horizon of fertile soils (Belyaeva, Haynes 2012), or even higher than in black earth (Chodorowski et al. 2019, Łabaz et al. 2019). The TOC:TN ratios in surface layers SII–SIV were very close (12.5-13.9, Table 2), while that of SI was much higher (18.9) because of a significant content of nitrogen-free components (over 60 vol.%, Table 1). As above, in the humus horizon of good quality soil, the TOC:TN ratio is in the range 10-13 (Ostrowska, Porębska

Table 3

The chemical properties of surface layers (S) and ash-slag subsoils (A)

Type of material	Soil				WEOM			
	pH_{KCl}	TOC	TN	TOC:TN	$CaCO_3$	WEOC	WETN	WEOC:WETN
		(%)			(%)	(mg dm^{-3})		
Surface layers								
SI	7.44	3.11	0.17	18.9	1.00	63.07	7.58	8.3
SII	6.75	3.18	0.26	12.5	0.93	86.58	17.38	5.0
SIII	6.99	4.40	0.32	13.8	1.39	88.16	14.41	6.1
SIV	6.66	4.77	0.36	13.4	0.80	86.57	20.78	6.6
Ash-slag subsoils layers								
AI	8.55	2.44	0.05	53.4	2.42	33.93	2.52	13.5
AII	8.16	2.30	0.05	47.8	3.14	24.61	5.41	4.6
AIII	8.45	2.17	0.05	47.5	2.51	36.10	6.19	5.8
AIV	8.37	2.36	0.05	50.8	3.17	28.23	5.98	4.7

TOC – total organic carbon, TN – total nitrogen, WEOM – water-extractable organic matter, WEOC – water extractable organic carbon, WETN – water extractable total nitrogen

2015, Błońska et al. 2017, Matschullat et al. 2018), so the values determined in surface layers SII–SIV were favorable for plants and soil microorganisms. For ash-slag subsoils (A), the TOC:TN ratios were high and ranged from 48 to 53 (Table 3), which informed about great domination of carbon over nitrogen. For different ashes left after combustion of coal in the Ruhr Area, the values of TOC:TN ratios varied from 39 to 50, while this ratio in slag was 24 (Hiller 2000). High TOC:TN ratios are also characteristic of fly ashes, which contain different but high amounts of carbon and very low amounts of nitrogen (Haynes 2009). The lowest contents of WEOC and WETN and the widest range of WEOC:WETN values were noted in surface layer SI. In the other surface layers (SII–SIV), the content of WEOC (86.6-88.2) and WETN (14.4-20.8) was higher and the WEOC:WETN ratio was narrower (5.0-6.6) in WEOM (Table 3). A similar diversity of the content of nitrogen and the values of WEOC:WETN ratio were measured in subsoil layers (S). It should be attributed to the compositions of surface layers SII–SIV, which contained 75.0-87.5 vol.% of organic substrates. The wider range of TOC:TN values in surface layer SI (in the soil and in WEOM) may lead to increased mobility of carbon compounds and their increased migration to the subsoil. It is in agreement with the study by Bielińska and Futa (2009), run on the same experimental object a few years before our studies. The activity of the enzymes determined in the study was greater in surface layers SII–SIV, enriched in fermented municipal sewage, than in surface layer SI. The high activity of enzymes in surface layers S II-IV could also be linked to their neutral pH, while basic pH of SI may restrict the metabolic activity of microorganisms (Table 3).

XRD analysis of surface layers and ash-slag subsoils

Figures 1*a* and 1*b* show the powder X-ray diffraction patterns of SII–SIV and AII–AIV samples, respectively. XRD analysis of SI–SIV materials

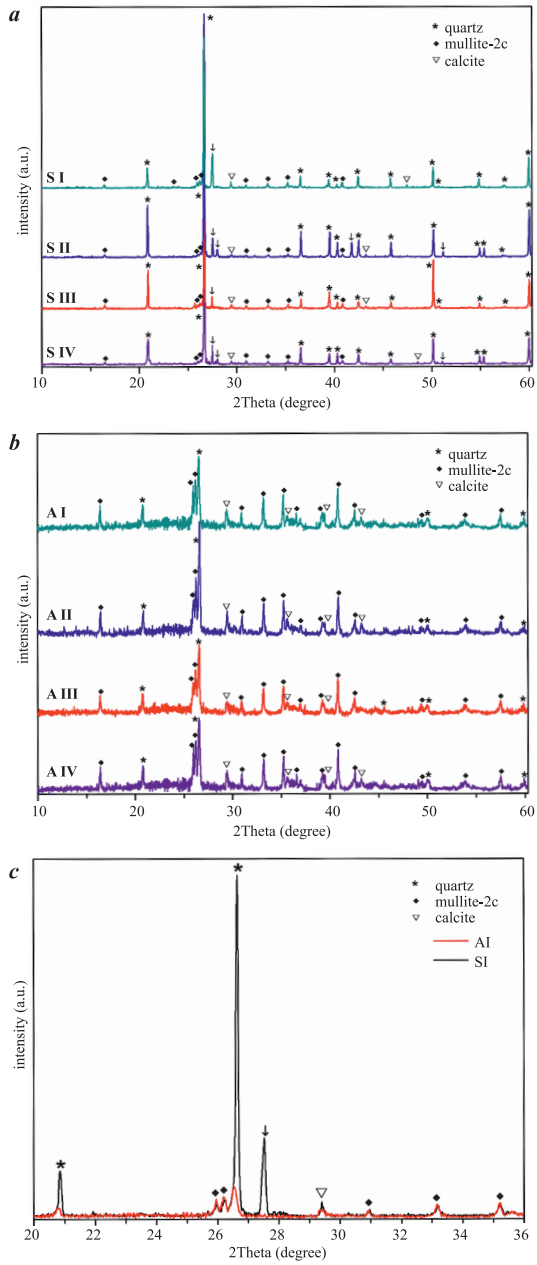

Fig. 1. X-ray diffraction patterns of: *a* – samples SI–SIV, *b* – samples AI–AIV, *c* – sample SI and sample AI in the range of 2Theta from 20° to 36°

showed the presence of quartz (hexagonal SiO_2, JCPDS #01-070-7345, marked as*), mullite-2c (orthorhombic $Na_{0.01}Mg_{0.05}Al_{8.52}Fe_{0.29}Si_{3.13}Ti_{0.02}O_{19.55}$, JCPDS #00-072-0060 (Lanz et al. 2020), marked as ◆) as well as calcite (rhombohedral $CaCO_3$, JCPDS #01-071-3699, marked as ∇) – Figure 1*a*. Moreover, for all surface layer samples (S), we observed the presence of additional diffraction lines (marked as ↓), which after detailed analysis could be assigned to one of the following two aluminosilicates: $NaAl_3Si_3O_{11}$ (JCPDS #00-046-0740) or $Na_{0.85}K_{0.15}AlSi_3O_8$ (JCPDS #01-075-1635). The intensities of peaks corresponding to individual phases differ significantly. The diffraction lines attributed to quartz show the highest intensity, which indicates that the mass fraction of this phase in the SI–SIV samples was dominant (Figure 1*a*).

The powder diffraction patterns of AI–AIV materials consisted of diffraction lines which can be assigned to quartz, mullite-2c and calcite (Figure 1*b*) only. Unlike previous samples, the intensities of the observed diffraction peaks assigned to quartz as well as mullite-2c are close to each other. This can indicate that the mass fraction of both phases in AI–AIV samples is comparable. The content of calcite was low, which is confirmed by the low intensities of the diffraction lines corresponding to this compound.

In conclusion, the quantitative compositions of the surface layers and ash-slag subsoil samples differ significantly from each other. It is clearly visible in Figure 1c, where the powder diffraction patterns of SI and AI samples are shown together. The very high intensity of the peaks corresponding to quartz clearly indicates that this phase is dominant in SI–SIV materials.

Spectroscopic characterization of WEOM fractions

UV-Vis analysis

The spectra of S samples indicate a significantly higher absorbance than the spectra of A samples. The course of the absorption spectra of S samples was smoother and the intensity of their absorbance decreased in the order: SIV > SII ≥ SIII > SI. The course of the absorption spectra of A samples was steep and monotonous, and the absorption intensity was relatively low.

The spectra of S samples show a characteristic band at 270-290 nm, related to the π-π* electronic transition characteristic of phenolic and quinone structures, derivatives of benzoic acid and/or polycyclic aromatic hydrocarbons of two or more rings, which indicates more aromatic character of WEOM-S than WEOM-A. The ability of A samples to absorb electromagnetic radiation is poor, the strongest absorption was observed for the groups absorbing radiation from the short wavelength part of the spectrum, but still the number of chromophores capable of absorption in this range is small compared to that of S samples. .

These observations are confirmed by the values of absorption coefficients (Table 4). The aromaticity index $SUVA_{254}$ of WEOM takes much higher values for surface layers than for subsoils. This result may be explained

Table 4

Absorption coefficients of WEOM

Type of material	$SUVA_{254}$	ΔlogK	$E_{254}:E_{365}$
Surface layers			
SI	1.88	1.30	5.15
SII	2.44	1.32	4.74
SIII	2.11	1.33	4.65
SIV	4.70	1.34	4.64
Ash-slag subsoils layers			
AI	0.45	0.81	6.20
AII	0.42	0.80	7.05
AIII	0.32	0.81	7.09
AIV	0.52	1.03	7.05

$SUVA_{254}$ – specific absorbance coefficient calculated as the absorbance at 254 nm and WEOC value (mg L^{-1}), corrected against the cuvette length (m), ΔlogK – the difference of logarithms of absorbance at the wavelengths of 400 nm and 600 nm, respectively, $E_{254}:E_{365}$ – calculated as the absorbance at 250 nm to the absorbance of 365 nm

by the presence of decomposition products of organic waste deposited on the surface layers of the soil. Higher values of this index are related to a greater contribution of aromatic groups and compounds of greater molecular mass (Weishaar et al. 2003, Corvasce et al. 2006, Chowdhury 2013, Wang et al. 2020). The results suggest that WEOM from the surface layers is more humified than that from subsoils (Ma et al. 2021).

According to the ΔlogK values, which varied between 0.80-1.03 and 1.30-1.34 for A and S samples respectively, the OM considered is moderately and poorly humified (Kumada 1987), which can be interpreted as a consequence of the short duration of the process (12 years). Lower ΔlogK values for A samples imply preferential migration of structurally simple particles into deeper profile layers. On the other hand, S samples are richer in OM, more chemically complex and more aromatic. The $E_{280}:E_{365}$ ratio is related to molecular mass and degree of humification; its lower value implies the presence of compounds of greater molecular mass and a greater degree of decomposition of parent compounds (Peuravuori, Pihlaja 1997, Wang et al. 2009). According to Waldrip et al. (2022), compounds of greater molecular mass may adsorb to the soil minerals in the surface layers and help maintain nutrients in these layers, whereas OM of low molecular mass may migrate to deeper layers of the soil profile more easily.

Analysis of the UV-Vis spectra obtained also informs about the impact of additives applied to stimulate recultivation, which is particularly well seen in S samples. The strongest effect on the S samples properties was produced by the addition of sewage sludge and bark; however, irrespectively of which

of the above additions had been introduced, the addition of ash lead to a significant reduction in light absorption (Figure 2). The higher $SUVA_{254}$ together with the lower E_{254}:E_{365} in the SIV sample than the corresponding values in the other surface layers indicated that this sample contained aromatic groups of much higher molecular mass. Similarly, the lowest values of $SUVA_{254}$ together with the higher values of E_{254}:E_{365} obtained in the sample collected at site SI indicated lower complexity of this material and its less condensed (aromatic) character (Ma et al. 2021).

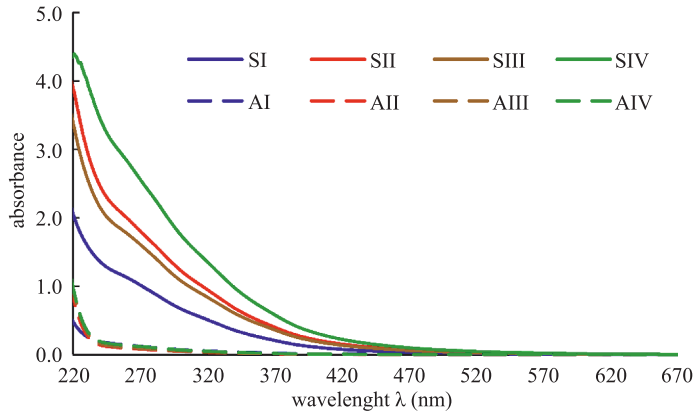

Fig. 2. The UV-Vis spectra of water extractable organic matter (WEOM) from samples of surface layers (SI–SIV) and ash-slag subsoils (AI–AIV)

EEM fluorescence spectra

Analysis of the EEM fluorescence spectra of S and A samples allowed identification of the four main fluorescence regions (Figure 3): P1 with max $\lambda_{Ex/Em}$ = 230 nm/340 nm, P2 with $\lambda_{Ex/Em}$ = 275 nm/330 nm, P3 as a double maximum, upon excitation at λ_{Ex} = 240 and 300 nm, a well-defined maxi-

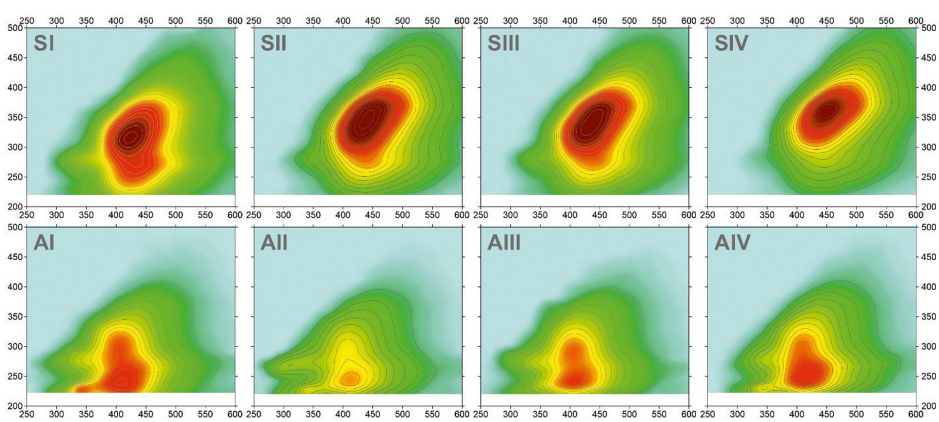

Fig. 3. The EEM spectra of water extractable organic matter (WEOM) from surface layers (S I-IV) and ash-slag subsoils (A I-IV) samples

mum of emission at λ_{Em} = 400/410 nm and P4 as a double maximum upon excitation at λ_{Ex} = 300 nm and 340 nm, corresponding to the maximum emission of λ_{Em} = 425 nm.

The fluorescence peaks P1 and P2 occur mainly in the WEOM-A spectra. According to literature (Chen et al. 2003, Wu et al. 2012, Mielnik, Kowalczuk 2018), P1 and P2 areas have been assigned to the biodegradable components characteristic of dissolved microbial metabolites, and correspond to the fluorescence of components of simple structures and low molecular mass. The presence of P1 and P2 in the spectra of WEOM-A suggests the domination of amino acids in proteins in the WEOM from subsoils. The content of protein-like components is often used as an indicator of DOM lability and bacterial productivity (Hudson et al. 2007). In the spectra of WEOM-S, peaks P1 and P2 are not faintly visible. For samples S and A, the characteristic area is peak P3, related to the presence of biologically unstable OM, rich in aliphatic carbon originating from fulvic-like matter decomposition (Yamashita et al. 2008, He et al. 2015).

In the spectra of S samples, the main fluorescence maximum appears in P4 area, while in the spectra of A samples it is very weak or absent. The fluorescence area with P4 maximum corresponds to the fluorescence of more humified structures, not subjected to biodegradation of soil organic compounds, and may be assigned to the presence of high-molecular components of linearly condensed aromatic ring systems with electron-acceptor substituents (Mielnik et al. 2021). The observations are fully consistent with the data on the development of diversity of OM forms, which would indicate that particular phases making individual fractions permeate due to chemical interrelations.

The values of HIX, BIX, f_{450}/f_{500} and $\Sigma IFl_{465}/a_{465}$ coefficients were determined on the basis of the EEM spectra and presented in Figure 4. The values of f_{450}/f_{500} and BIX slightly increased down the profile. In contrast to these, the values of HIX and $\Sigma IFl_{465}/a_{465}$ rapidly decreased with increasing profile depth, at each site studied. However, all the parameters remained relatively unchanged in all layers of the soil profile at all sites.

The higher HIX values for S samples indicated that they had a higher degree of humification than A samples (3.3-4.7) (Zsolnay et al. 1999). Higher values of HIX obtained in S samples indicate that surface layers contain more condensed polymers of greater molecular mass, while a lower HIX in A samples informs that the subsoil contains OM more susceptible to microbiological decomposition (Xu et al. 2013, Wardinski et al. 2022). These results are in agreement with those from an analysis of the humification index $\Sigma IFl_{465/}a_{465}$ used for evaluation of the degree of intramolecular transformation of humus substances (Milori et al. 2002). Higher values of $\Sigma IFl_{465/}a_{465}$ obtained for S samples are related to the progress in surface humification and a higher degree of intramolecular transformation.

The values of BIX varied from 0.40 to 0.96 (Figure 4) and according

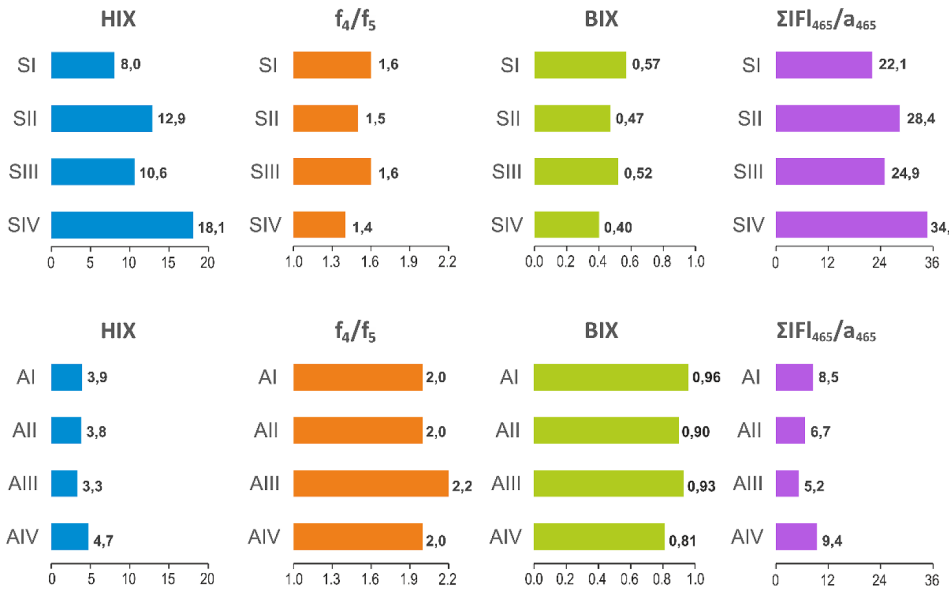

Fig. 4. The values of fluorescence coefficients (HIX, BIX, f_{450}/f_{500} and $\Sigma IFl_{465}/a_{465}$), based on fluorescence spectral data

to literature, they fall in the range of values reported for natural DOM in aquatic environment (Mielnik, Kowalczuk 2018). High values of BIX (>1.0) are characteristic of the environments of high biological activity and usually are indicative of OM of indigenous origin and the presence of recently produced DOM (He et al. 2015). The values of BIX from 0.81 to 0.96 obtained for A samples, correspond to recently produced WEOM of biological or microbiological origin. This result is consistent with the identified EEM components and indicates an increase in the content of simple protein-like components in A samples.

The f_{450}/f_{500} coefficient, proposed by McKnight et al. (2001), has been widely used for differentiation between WEOM from land resources and that of microbiological origin, as it is expected that organic compounds from land resources contain more coupled aromatic structures than substances of microbiological origin. The f_{450}/f_{500} value of 1.4 or lower corresponds to DOM from land resources, whereas the values of 1.9 or higher indicate the material of microbiological origin (Birdwell et al. 2010). The higher values of f_{450}/f_{500} for A samples testify to the prevalence of OM of microbiological origin, in contrast to S samples.

As follows from the analysis of the fluorescence indices obtained in the study, the components of A subsoil samples, made of ash-slag, are mainly of biological or microbiological origin, confirmed by a continuous flow of root biomass, root secretion, and slow inflow of simple aerial residues. The components of WEOM from surface layers were of a more complex and more aromatic character.

Delayed luminescence

The use of DL in investigation of DOM may provide additional information on the structure and photoreactivity of its components.

The values of the intensities of DL recorded for the solutions of WEOM from S and A samples are presented in Figure 5. As seen in this figure,

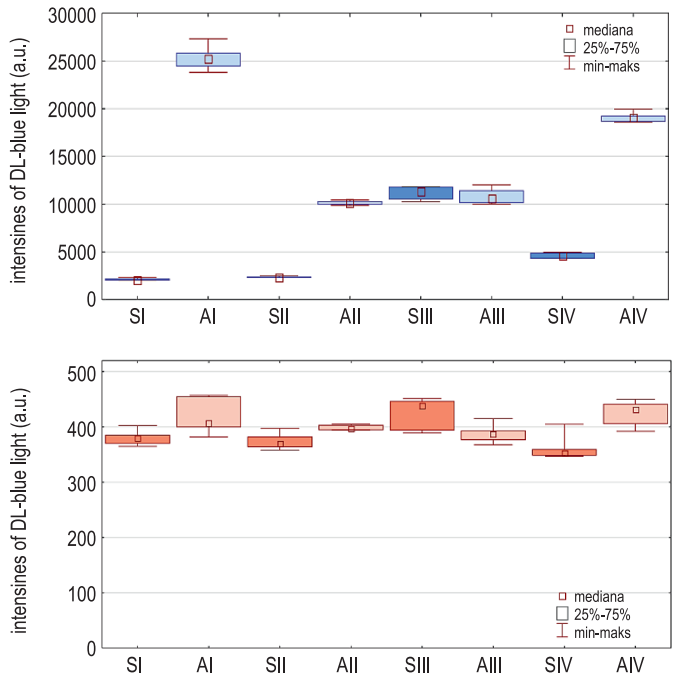

Fig. 5. Intensities of delayed luminescence excited by blue (DL-blue) and red (DL-red) light

the WEOM solutions studied show different abilities to emit radiation in the DL mode, depending significantly on the conditions of OM transformation. Upon excitation with blue light, of the greatest energy, the DL intensity was higher for WEOM-A than WEOM-S. Upon excitation with red light, no considerable differences in DL intensity were observed. These results indicate the presence of different numbers or different qualities of centers (groups) capable of generating DL as well as initiation of different mechanisms stimulated by the interaction of the applied radiation with the OM molecules. The latter may reflect different distribution of luminophores in the structures of the material studied and their different photoreactivities.

There is a large diversity of mechanisms leading to DL initiation. Moreover, as follows from the study by Mielnik and Asensio (2018), the mechanisms leading to DL emission upon excitation with blue light may be different than those active upon excitation with red light. In general, the DL emission may be a result of radical processes stimulated by excited quinones,

which may act as sensitizers for the neighboring fragments of OM biopolymers. Besides, aromatic amino acids and/or nucleic bases may show also high photoreactivity and photoluminescence.

CONCLUSIONS

The use of UV-Vis spectroscopy and luminescence spectroscopy (fluorescence and delayed luminescence) has brought about a new outlook on the photoluminescence properties of WEOM, which has contributed to reflecting a real complexity of processes involved in formation and transformations of the soil OM. They permitted effective investigation of the properties and migration of WEOM from the surface layers richer in OM, towards deeper layers of the profile, made of ash-slag mixture.

The studied WEOM was poorly humified, which can be explained by a short time of humification process (12 years). While the WEOM fraction of higher molecular mass has been retained in the surface layer. Thus, the surface layer is richer in WEOM showing more complex chemical structure and greater aromaticity. The presence of WEOC in the ash-slag subsoil layer results of the washing out of WEOM particles from the surface layers. The particles of simple structure and low molecular mass are preferentially transported into deeper layers of the profile. Moreover, a considerable content of WEOM in the ash-slag layer may be a consequence of the activity of microorganisms and the release of DOM from plant roots.

The obtained results showed, that the dissolved OM transportation to deeper layers of the soil profile depends on the type of OM and chemical and mineral composition of different horizons.

Author contributions

L.M. – writing – original draft preparation, methodology, results and discussion, T.T. – writing – review & methodology, J.C. – writing methodology, results & discussion, E.T. – writing, XRD analyzes, M.P. – graphical preparation of results, E.H. – review and editing . All authors have read and agreed to the published version of the manuscript.

Conflicts of interest

Funding: This research received no external funding.

REFERENCES

Belyaeva, O.N., Haynes, R.J. (2012) 'Comparison of the effects of conventional organic amendments and biochar on the chemical, physical and microbial properties of coal fly ash as a plant growth medium', *Environmental Earth Sciences*, 6, 1987-1997, available: https://doi.org/10.1007/s12665-011-1424-y

Bielińska, E.J., Futa, B. (2009) 'Organic matter effect on biochemical transformations in anthropogenic soils in power plant ash dumping ground', *Soil Science Annual*, 60, 18-26 (in Polish)

Birdwell, J.E., Summers Engel, A. (2009) 'Characterization of dissolved organic matter in cave and spring waters using UV–Vis absorbance and fluorescence spectroscopy', *Organic Geochemistry*, 41(1), 270-280, available: https://doi.org/10.1016/j.orggeochem.2009.11.002

Bolan, N.S., Adriano D.C., Kunhikrishnan, A., Trevor, J., McDowell, R., Senesi, N. (2011) 'Chapter One - Dissolved Organic Matter: Biogeochemistry, Dynamics, and Environmental Significance in Soils', *Advances in Agronomy*, 110, 1-75, available: https://doi.org/10.1016/B978-0-12-385531-2.00001-3

Chen, W., Westerhoff, P., Leenheer, J.A., Booksh, K. (2003) 'Fluorescence excitation – emission matrix regional integration to quantify spectra for dissolved organic matter', *Environmental Science & Technology*, 37, 5701-5710.

Chowdhury, S. (2013) 'Trihalomethanes in drinking water: Effect of natural organic matter distribution', *Water SA*, 39, 1-7, available: https://doi:10.4314/wsa.v39i1.1

Corvasce, M., Zsolnay, A., D'Orazio, V., Lopez, R., Miano, T.M. (2006) 'Characterization of water extractable organic matter in a deep soil profile', *Chemosphere*, 62, 1583-1590, available: https://doi.org/10.1016/j.chemosphere.2005.07.065

Czyż, H., Kitczak, T. (2007) 'Suitability of some grass mixtures sown on various substrates containing ash and organic matter for lawns', *Quarterly of Environmental Engineering and Design*, 133, 68-75 (in Polish)

Daouk, S., Frege, C., Blanc, N., Mounier, S., Redon, R., Merdy, P., Lucas, Y., Pfeifer, H-R. (2015)' Fluorescence spectroscopy to study dissolved organic matter interactions with agrochemicals applied in Swiss vineyards', *Environmental Science and Pollution Research*. 22, 9284-9292, available: https://doi.org/10.1007/s11356-015-4086-6

Gao, J., Liang, C., Shen, G., Lv, J., Wu, H. (2017) 'Spectral characteristics of dissolved organic matter in various agricultural soils throughout China', *Chemosphere*, 176, 108-116, available: https://doi:10.1016/j.chemosphere

Gao, L., Zhou, Z., Reyes, A.V., Guo, L. (2018) 'Yields and characterization of dissolved organic matter from different aged soils in northern Alaska', *Journal of Geophysical Research: Biogeosciences*, 123, 2035-2052, available: doi.org/10.1029/2018JG004408

Gaskin J. (2020) 'Benefits of Increasing Soil Organic Matter'. Chapter 3: Benefits of Increasing Soil Organic Matter. In Conservation Tillage Systems in the Southeast: Production, Profitability and Stewardship, Bergtold, J., Sailus, M., Eds., SARE handbook, series 15, ISBN 978-1-888626-18-6. www.sare.org/conservation-tillage-in-the-southeast

Gerke, J. (2022) 'The Central Role of Soil Organic Matter in Soil Fertility and Carbon Storage', *Soil Systems*, 6, 33, available: https://doi.org/10.3390/soilsystems6020033

Haynes, R.J. (2009) 'Reclamation and revegetation of fly ash disposal sites – Challenges and research needs', *Journal of Environmental Management*, 90, 43-53, available: https://doi.org/10.1016/j.jenvman.2008.07.003

He, Q., Li Gao, L., Wang, Z., Tang, Y., Pan, B., Li, M. (2021) 'Fluorescence characteristics of dissolved organic matter in several independent water bodies: possible sources and land-use effects', *Environmental Science and Pollution Research*, 28, 33241-33253, available: https://doi.org/10.1007/s11356-021-12972-0

He, X-S, Xi, B-D, Gao, R-T, Wang, L., Ma, Y., Cui, D-Y, Tan, W-B. (2015) ' Using fluorescence spectroscopy coupled with chemometric analysis to investigate the origin, composition, and dynamics of dissolved organic matter in leachate-polluted groundwater', *Environmental Science and Pollution Research*, 22, 8499-8506, available: https://doi.org/10.1007/s11356-014-4029-7

Hiller, D.A. (2000) 'Properties of Urbic Anthrosols from an abandoned shunting yard in the Ruhr area, Germany', *Catena*, 39, 245-266, available: https://doi.org/10.1016/S0341-8162(00)00081-3

Hudson, N., Baker, A., Reynolds, D. (2007) 'Fluorescence analysis of dissolved organic matter in natural, waste and polluted waters – a review', *River Research and Applications*, 23, 631-649, available: https://doi.org/10.1002/rra.1005

Kaiser, K., Guggenberger, G. (2000) 'The role of DOM sorption to mineral surfaces in the preservation of organic matter in soils', *Organic Geochemistry*, 31, 7-8, 711-725, available: https://doi.org/10.1016/S0146-6380(00)00046-2

Khan, I., Umar, R. (2019) 'Environmental risk assessment of coal fly ash on soil and groundwater quality, Aligarh, India', *Groundwater for Sustainable Development*, 8, 346-357, available: https://doi.org/10.1016/j.gsd.2018.12.002

Kumada, K. (1987) 'Chemistry of soil organic matter', Japan Scientific Societies Press, Elsevier, Tokyo.

Łabaz, B., Kabała, C., Dudek, M., Waroszewski, J. (2019) 'Morphological diversity of chernozemic soils in south-western Poland', *Soil Science Annual*, 70, 211-224, available: https://doi:10.2478/ssa-2019-0019

Lanz, S., Brikenstock, J., Fischer, L., Schneider, H., Fischer, R. (2020) 'Mullite-2c – a natural polytype of mullite', *European Journal of Mineralogy*, 32, 235-249, available: https://doi:10.5194/ejm-32-235-2020

Ma, W., Li, Z., Ding, K., Zhou, Q. (2021) 'Dynamics of water extractable organic carbon at a subtropical catchment using fluorescence excitation-emission matrix spectroscopy coupled with parallel factor analysis', *European Journal of Soil Science*, 72, 871-885, available: https://doi.org/10.1111/ejss.13006

Matschullat, J., Reimann, C., Birke, M., dos Santos Carvalho, D. (2018) 'GEMAS: CNS concentrations and C/N ratios in European agricultural soil', *Science of the Total Environment*, 627, 975-984, available: https://doi.org/10.1016/j.scitotenv.2018.01.214

McKnight, D.M., Boyer, E.W., Westerhoff, P.K., Doran, P.T., Kulbe, T., Andersen, D.T. (2001) 'Spectrofluorometric characterization of dissolved organic matter for indication of precursor organic material and aromaticity', *Limnology and Oceanography*, 46(1), 38-48, available: https://doi.org/10.4319/lo.2001.46.1.0038

Mielnik, L., Asensio, C. (2018) 'Using delayed luminescence to characterize humic acids from lake sediments', *Journal of Soils and Sediments*, 18, 2844-2850, available: https://doi.org/10.1007/s11368-018-1914-6

Mielnik, L., Kowalczuk, P. (2018) 'Optical characteristic of humic acids from lake sediments by excitation-emission matrix fluorescence with PARAFAC model', *Journal of Soils and Sediments*. 18, 2851-2862, available: https://doi.org/10.1007/s11368-018-1947-x

Mielnik, L., Weber, J., Podlasiński, M., Kocowicz, A. (2021) 'Fluorescence properties of humic substances transformed in ectohumus horizons of Podzols affected by alkaline fly-ash', *Land Degradation and Development*, 32, 3487-3497, available: https://doi:10.1002/ldr.3926

Milori, D.M.B.P., Neto, L.M., Bayer, C., Mielniczuk, J., Bagnato, V.S. (2002) 'Humification degree of soil humic acids determined by fluorescence spectroscopy', *Soil Science*, 167, 739-749, available: https://doi:10.1097/00010694-200211000-00004

Pandey, V.C. (2012) 'Invasive species based efficient green technology for phytoremediation of fly ash deposits', *Journal of Geochemical Exploration*, 123, 13-18, available: https://doi.org/10.1016/j.gexplo.2012.05.008

Pandey, V.C. (2020) 'Scope of fly ash use in agriculture: prospects and challenges". In: Pandey, V.C., (Ed.) Phytomanagement of Fly Ash. Elsevier, Amsterdam, pp. 63-101, available: https://doi:10.1016/B978-0-12-818544-5.00003-1

Peuravuori, J., Pihlaja, K. (1997) 'Molecular size distribution and spectroscopic properties of aquatic humic substances', *Analytica Chimica Acta*, 337, 2, 133-149, available: https://doi.org/10.1016/S0003-2670(96)00412-6

Pierzyna, P. (2017) 'Disposal of coal combustion wastes in the hydraulic backfill process", IOP Conference Series: Materials Science and Engineering 268, 012011, available: https://doi:10.1088/1757-899X/268/1/012011

Prokowski, Z., Mielnik, L. (2012) 'Application of the Long-Term Delayed Luminescence for Study of Natural Water Environments'. In Marcelli M., (Ed.) Oceanography. InTech, Rijeka, pp. 79-94, available: doi:10.5772/28478

Ram, L.C., Masto, R.E. (2014) 'Fly ash for soil amelioration: A review on the influence of ash blending with inorganic and organic amendments', *Earth-Science Reviews*, 128, 52-74, available: http://dx.doi.org/10.1016/j.earscirev.2013.10.003

Rees, M.R., Parker, J.P. (2005) 'Filtration increases the correlation between water extractable organic carbon and soil microbial activity', *Soil Biology and Biochemistry*, 37, 12, 2240-2248, available: https://doi.org/10.1016/j.soilbio.2005.03.024

Shaheen, S.M., Hooda, P.S., Tsadilas, Ch.D. (2014) 'Opportunities and challenges in the use of coal fly ash for soil improvements – A review', *Journal of Environmental Management*, 145, 249-267, available: https://doi.org/10.1016/j.jenvman.2014.07.005

Shon, Ch-S, Saylak, D., Zollinger, D.G. (2009) 'Potential use of stockpiled circulating fluidized bed combustion ashes in manufacturing compressed earth bricks', *Construction and Building Materials*, 23, 2062-2071, available: https://doi.org/10.1016/j.conbuildmat.2008.08.025

Singh, K., Pandey, V.C., Singh, B., Patra, D.D., Singh, R.P. (2016) 'Effect of fly ash on crop yield and physico-chemical, microbial and enzyme activities of sodic soils', *Environmental Engineering and Management Journal*, 15, 2433-2440, available: https://doi:10.30638/eemj.2016.266

Skousen, J., Ziemkiewicz, P., Yang, J.E. (2012) 'Use of coal combustion by-products in mine reclamation: review of case studies in the USA', *Geosystem Engineering*, 15, 71-83, available: https://doi.org/10.1080/12269328.2012.676258

Šulc, R., Šídlová, M., Formáček, P., Snop, R., Škvára, F., Polonská, A. (2022) 'A study of physicochemical properties of stockpile and ponded coal ash', *Materials*, 15(10), 3653, available: https://doi.org/10.3390/ma15103653

Szwalec, A., Mundała, P., Kędzior, R. (2022) 'Suitability of selected plant species for phytoremediation: A case study of a coal combustion ash landfill', *Sustainability*, 14(12), 7083, available: https://doi.org/10.3390/su14127083

Uzarowicz, Ł., Zagórski, Z., Mendak, E., Bartmiński, P., Szara, E., Kondras, M., Oktaba, L., Turek, A., Rogoziński, R. (2017) 'Technogenic soils (Technosols) developed from fly ash and bottom ash from thermal power stations combusting bituminous coal and lignite. Part I. Properties, classification, and indicators of early pedogenesis', *Catena*, 157C, 75-89, available: https://doi.org/10.1016/j.catena.2017.05.010

Waldrip, H., Schwartz, R. C., He, Z., Todd, R.W., Baumhardt, R.L., Zhang, M., Parker, D., Brauer, D., Min, B.R. (2022) 'Soil water extractable organic matter under long-term dryland cropping systems on the Texas High Plains', *Soil Science Society of America Journal*, 86, 1249-1263, available: https://doi.org/10.1002/saj2.20432

Wang, D. , Peng, Q., Yang, W.X., Dinh, Q.T., Tran, T.A.T., Zhao, X.D., Wu, J.T., Liu, Y.X., Liang, D.L. (2020) 'DOM derivations determine the distribution and bioavailability of DOM-Se in selenate applied soil and mechanisms', *Environmental Pollution*, 259, 113899, available: https://doi.org/10.1016/j.envpol.2019.113899

Wang, L., Wu, F., Zhang, R., Li, W., Liao, H. (2009) 'Characterization of dissolved organic matter fractions from Lake Hongfeng, Southwestern China Plateau', *Journal of Environmental Sciences*, 21, 5, 581-588, available: https://doi.org/10.1016/S1001-0742(08)62311-6

Wardinski, K.M., Hotchkiss, E.R., Jones, C.N., McLaughlin, D.L., Strahm, B.D., Scott, D.T. (2022) 'Water-soluble organic matter from soils at the terrestrial-aquatic interface in wetland-dominated landscapes', *Journal of Geophysical Research: Biogeosciences*, 127, e2022JG006994, available: https://doi.org/10.1029/2022JG006994

Weber, J., Strączyńska, S., Kocowicz, A., Gilewska, M., Bogacz, A., Gwiżdż, M., Dębicka, M. (2015) 'Properties of soil materials derived from fly ash 11 years after revegetation of post-mining excavation', *Catena*, 133, 250-254, available: https://doi.org/10.1016/j.catena.2015.05.016